6
Temporal quantum correlation in the light of NOνA and T2K anomaly

This chapter presents the findings of ref. [140]. The two long-baseline accelerator experiments, NOνA and T2K released data for δ_{CP} [342, 343]. Their experimental result depicts a mismatch for normal ordering. NOνA prefers $\delta_{CP} \sim 0.8\pi$, while T2K governs CP phase value 1.4π. These two assessments are in disagreement, exceeding 90% C.L. with two degrees of freedom. While results for inverse ordering are matched, the non-zero value of the CP phase parameter in T2K and the mismatch with NOνA in the mass matrix suggest that complexity is present not only in the mass matrix but can also in new physics. Several new physics solutions have been proposed to address the anomalies observed in T2K and NOνA, with a notable contribution from complex NSI [344–346]. The resolution of the discrepancy between NOνA and T2K crucially involves a new CP phase, particularly in the context of flavor-changing neutral current NSI, denoted as $\epsilon_{\alpha\beta}$ where α and β are not equal. In ref. [345], the off-diagonal NSI parameters $\epsilon_{e\mu}$ and $\epsilon_{e\tau}$ are considered, with a focus on their impact on the observed anomaly. The introduction of these NSI parameters provides an effective means to study the novel CP phase. The parameters $\epsilon_{e\mu}$ and $\epsilon_{e\tau}$ are best explored through long-baseline accelerator appearance experiments, while the investigation of $\epsilon_{\mu\tau}$ is found to be most effective when utilizing atmospheric neutrinos.

The existence of new physics also holds the potential to impact quantum correlations in neutrino oscillations. The influence of new physics can manifest through both temporal and spatial quantum correlations within a system. Bell's inequality primarily deals with corrections in measurements conducted on spatially distant systems [80]. In a parallel manner, Leggett and Garg developed a test analogous to Bell's inequality but with a focus on corrections in measurements made on a system at different points in time [87]. The Leggett-Garg theorem is based on the assumptions of macrorealism (MR) and noninvasive measurement (NIM). A violation of the Leggett-Garg inequality implies that either the system cannot be realistically described or it is impossible to measure the system without disturbing it. However, systems driven by principles of quantum mechanics unequivocally diverge from these [87, 88]. A less stringent criterion, referred to as the stationarity condition, is employed to formulate LGtI as a substitute for the NIM condition [347, 348]. Since neutrino measurements undermine the NIM assumption, such inequalities are preferred to analyze temporal correlation in neutrinos [98, 99]. Violation of temporal correlation in neutrino oscillations is verified using the oscillation MINOS and Daya Bay experiments [97, 107].

For the NSI parameters that can accommodate NOνA and T2K anomaly, we explore the violation of LGtI within the context of three-flavor neutrino oscillations. Our analysis focuses on LGtI violations in scenarios involving complex NSI with $\epsilon_{e\mu}$ or $\epsilon_{e\tau}$ coupling in long baseline accelerator experiments for normal and inverted mass ordering. In this chapter, we explore the impact of NSI on the potential violation of LGtI. To do so, we specifically examine complex NSI parameters, namely $\epsilon_{e\mu}$ and $\epsilon_{e\tau}$, which have been demonstrated to accommodate the existing anomalies observed in NOνA and T2K experiments [345].

The structure of this chapter is outlined as follows. In section 6.1, we provide a brief definition of LGtI pertinent to neutrino oscillations. The formalism of this work is the same as the formalism 5.2 discussed in the previous chapter 5. In the subsequent section 6.2, we present and discuss our results. The conclusions drawn from our findings are encapsulated in the final section, 6.3.

6.1 Leggett Garg type inequalities

Leggett-Garg inequalities are a measure of quantum correlation analogous to Bell inequalities that concern spatial quantum correlation measures. However, LGI is a temporal quantum correlation measure that measures the system's correlation at various instances of time [87]. LGI is based on two assumptions: (1) Macro-realism (2) Noninvasive measurement. According to MR, a macroscopic system that can access two or more macroscopically distinct states will always be available in one of these states. NIM asserts that it is possible to perform a measurement on a system without even disturbing its dynamics. LGI manifests the level up to which quantum mechanics is applied to many-particle systems that exhibit decoherence, i.e., it manifests macroscopic coherence. LGI also tests the notion of realism, implying that a physical system possesses a complete set of definite values for various parameters prior to and independent of measurement. Realism introduces the concept of hidden variable theory. The violation of LGI suggests that such hidden variable theory cannot be used as an alternative tool for the time evolution of quantum mechanics. The LGI parameter K_n can be expressed in terms of a linear combination of autocorrelation functions, as [98]:

$$\sum_{i=1,j=i+1}^{i=n-1} C\left(t_i, t_j\right) - C\left(t_1, n\right), \tag{6.1}$$

with $C(t_i, t_j) = \langle \hat{Q}(t_i)\hat{Q}(t_j)\rangle$, where $C(t_i, t_j)$ is the autocorrelation function, and the expectation value of an operator can be written as $\langle \hat{Q}(t_i)\hat{Q}(t_j)\rangle = Tr[\{\hat{Q}(t_i), \hat{Q}(t_j)\}\rho(t_0)]$. Here, the average is taken with respect to $\rho(t_0)$, initial state of the system at time $t = 0$, $\hat{Q}$ is a generic dichotomic operator, i.e., $\hat{Q} = \pm 1$, $\hat{Q}^+ = Q$ and $\hat{Q}^2 = 1$ with $\hat{Q} = 1$ if the system is in target state; otherwise, $\hat{Q} = -1$. For $n \geq 3$, if realism is satisfied, then the LGI parameter $K_n \leq n - 2$. For n=3, LG inequality can be written as

$$K_3 = C(t_1, t_2) + C(t_2, t_3) - C(t_1, t_3) \leq 1. \tag{6.2}$$

Since $C(t_2, t_3)$ depends on the complete measurement of the system, it destroys the NIM postulate. To overcome this, the NIM postulate is replaced by a weaker condition of stationarity. After applying the weaker condition of stationarity, the correlation function $C(t_i, t_j)$ depends on the time difference. Under the assumption that time interval $t_2 - t_1$ = $t_3 - t_2$ = t and $t_1 = 0$ the LGtI parameter (K_3) can be written as [88] :

$$K_3 = 2C(0, t) - C(0, 2t) \leq 1. \tag{6.3}$$

Three-flavor neutrino oscillation K_3 can be expressed in terms of neutrino oscillation probability as [97, 99]:

$$K_3 = 1 + 2P_{\alpha\beta}(2t, E) - 4P_{\alpha\beta}(t, E). \tag{6.4}$$

In the ultrarelativistic limit, $t = L$ the LGI parameter K_3 is given as:

$$K_3 = 1 + 2P_{\alpha\beta}(2L, E) - 4P_{\alpha\beta}(L, E). \tag{6.5}$$

Which shows experimental feasibility of LG function on using condition $P_{\alpha,\beta}(2L, E)$ = $P_{\alpha,\beta}(L, \tilde{E})$ with suitable choice of E and $\tilde{E}$ [97]. To analyze LGtI, we can follow the probability expressions discussed in formalism 5.2.

6.2 Results and Discussion

In this section, we examine the impact of NSI scenarios involving $\epsilon_{e\mu}$ and $\epsilon_{e\tau}$ on the temporal measurement of quantum correlations within the neutrino system, considering three distinct experimental setups: (1) T2K (E $\approx$ 0 to 6 GeV, L= 295 km), (2) NOνA (E $\approx$ 1 to 10 GeV, L= 810 km), and (3) DUNE (E $\approx$ 1 to 10 GeV, L= 1300 km).

Input Parameters	ordering	1σ range
$\delta m^2/10^{-5}$ ev^2	NO	[7.20 - 7.51]
	IO	[7.20 - 7.51]
$\sin^2\theta_{12}$	NO	[0.292 - 0.319]
	IO	[0.290 - 0.317]
$\Delta m^2/10^{-3}$ ev^2	NO	[2.453 - 2.514]
	IO	[2.434 - 2.495]
$\sin^2\theta_{13}$	NO	[0.0214 - 0.0228]
	IO	[0.0217 - 0.0230]
$\sin^2\theta_{23}$	NO	[0.498 - 0.0565]
	IO	[0.0517 - 0.0567]
δ/π	NO	[1.10 - 1.66]
	IO	[1.37 - 1.65]

Table 6.1.: Best fit values of input parameters [349].

These are long-baseline accelerator experiments with neutrino energy of the order of GeV and a baseline length of a few hundred kilometers. These experiments are sensitive to measure mass hierarchy (Δm^2_{31}), mixing angle (θ_{23}), and CP phase (δ_{CP}). The value of standard oscillation parameters given in table 6.1 has been taken from [349]. The value of NSI parameters has been extracted from global analysis of the appearance and disappearance channels of combined NOνA and T2K data [345]. The 1σ range of these parameters are given in table 6.2. Table 6.3 illustrates the energy range in all three accelerator experiments where K_3 surpasses its classical bound for three flavor neutrino oscillation for SM and NSI scenarios. The outcomes for LGtI violation within the 1σ range in various accelerator experiments are visualized in figure 6.1, with T2K at the top, NOνA in the middle, and DUNE at the bottom.

In figure 6.1, for the T2K experiment, for the NO, K_3 is consistently violated for energies above 1.3 GeV. K_3 values corresponding to the SM and NSI scenarios exhibit overlapping regions within the error bar. So, the effects are most evident when observing maximum deviations. In the presence of $\epsilon_{e\tau}$, the violation of K_3 increases up to 4% as compared to the SM within the energy range of 1 GeV to 2 GeV. For the IO, the violation of K_3 occurs consistently for an energy range exceeding 1.5 GeV. However, there is no significant distinction between SM and NSI scenarios.

For the NOνA experiment, in the realm of NO, K_3 is always violated above 3.5 GeV. In the presence of $\epsilon_{e\tau}$, the violation of K_3 increases up to 16% as compared to the SM within the energy range of 3.8 GeV to 4.5 GeV. While the maximum violation can be reached up to 22% for this scenario. For IO, above 6.5 GeV, K_3 always shows violation. For the energy region $(2.5-3.5)$ GeV only $\epsilon_{e\tau}$ shows violation. For the DUNE experiment, in NO, the consistent violation of K_3 is observed for energies above 6 GeV. In the presence of $\epsilon_{e\tau}$, the violation of K_3 increases up to 32% as compared to the SM within the energy range of 3.5 GeV to 6.5 GeV. While the maximum violation can be reached up to 40% for this scenario. Whereas violation enhanced up to 5% in the $\epsilon_{e\mu}$ scenario within the energy range of 3.5 GeV to 4.5 GeV. For IO, violation of K_3 occurs for SM and both NSI scenarios for $(1.2-1.5)$ GeV energy range. Within the error bar, the maximum deviation in violation of K_3 for $\epsilon_{e\mu}$ and $\epsilon_{e\tau}$ as compared to SM for $(1.6-2.2)$ GeV energy range is 5% and 15%, respectively. For IO above 8.5 GeV, K_3 always shows violation for the $\epsilon_{e\tau}$ scenario

mass ordering	NSI	$\epsilon_{\alpha\beta}$	$\phi_{\alpha\beta}/\pi$	δ_{CP}/π
NO	$\epsilon_{e\mu}$	[0.057 - 0.22]	[0.88 - 1.9]	[1.17 - 1.79]
IO	$\epsilon_{e\mu}$	[0 - 0.149]	[0 - 360]	[1.27 - 1.74]
NO	$\epsilon_{e\tau}$	[0.078 - 0.492]	[1.25 - 1.91]	[1.2 - 1.79]
IO	$\epsilon_{e\tau}$	[0 - 0.4]	[1.02 - 1.97]	[1.24 – 1.82]

Table 6.2.: 1σ range of NSI parameters and δ_{CP} used in our analysis [345].

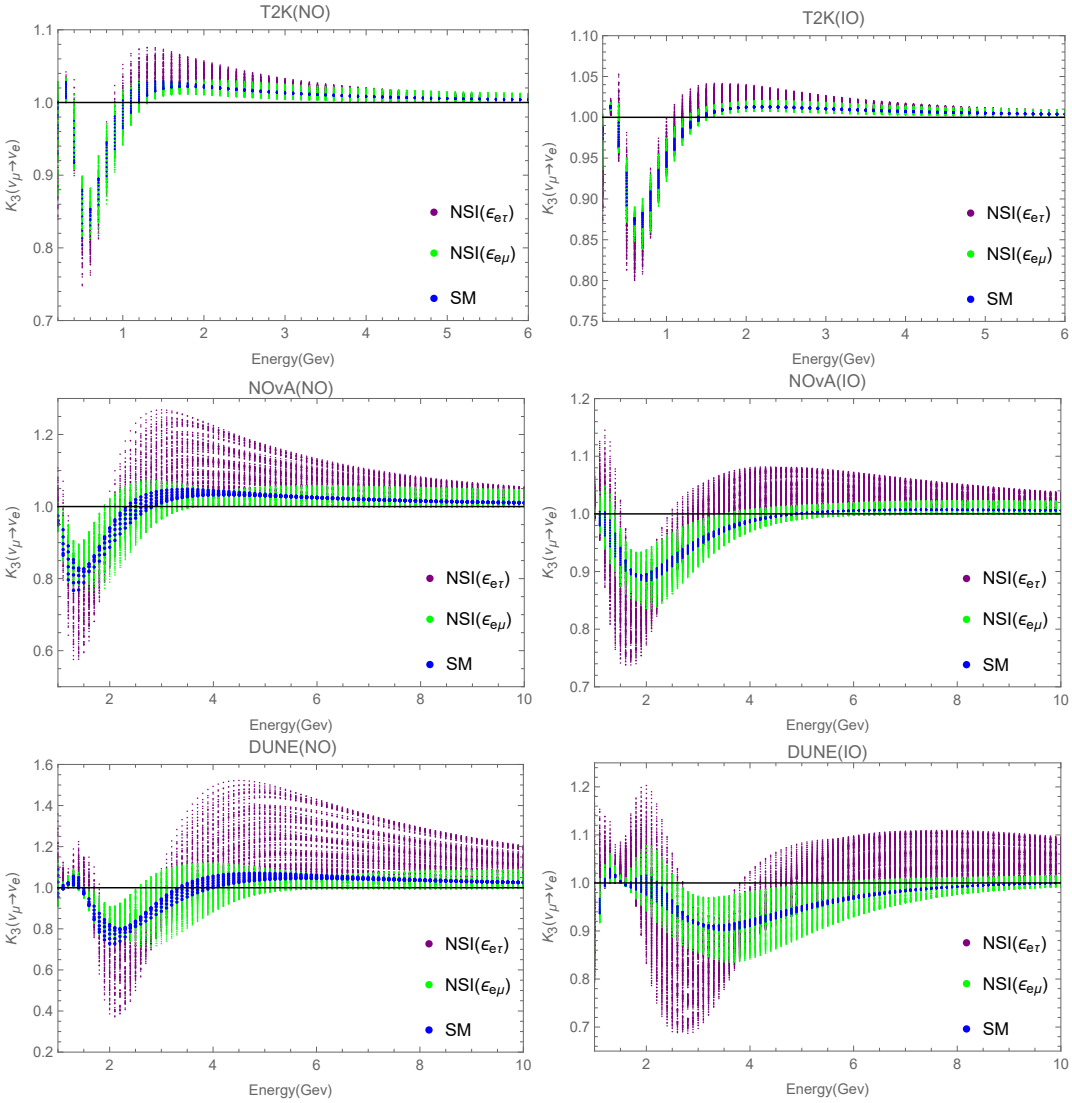

Figure 6.1.: Temporal quantum correlation, quantified in terms of LGtI (denoted as K_3), is plotted against neutrino energy for T2K, NOνA, and DUNE experiments. The green band represents LGtI with a 1σ allowed range of $\epsilon_{e\mu}$, $\phi_{e\mu}$, and cp phase; the purple band represents LGtI with 1σ an allowed range of $\epsilon_{e\tau}$, $\phi_{e\tau}$ and cp phase; and the blue band represents LGtI with 1σ an allowed range of cp phase.

within 1σ range, while SM does not show a violation. Therefore, the measurement of K_3 has the potential to discriminate among SM and $\epsilon_{e\tau}$ scenario, suggesting a potential indication of new physics. Additionally, within this range, the maximum enhancement in K_3 is 10% for the $\epsilon_{e\tau}$ scenario.

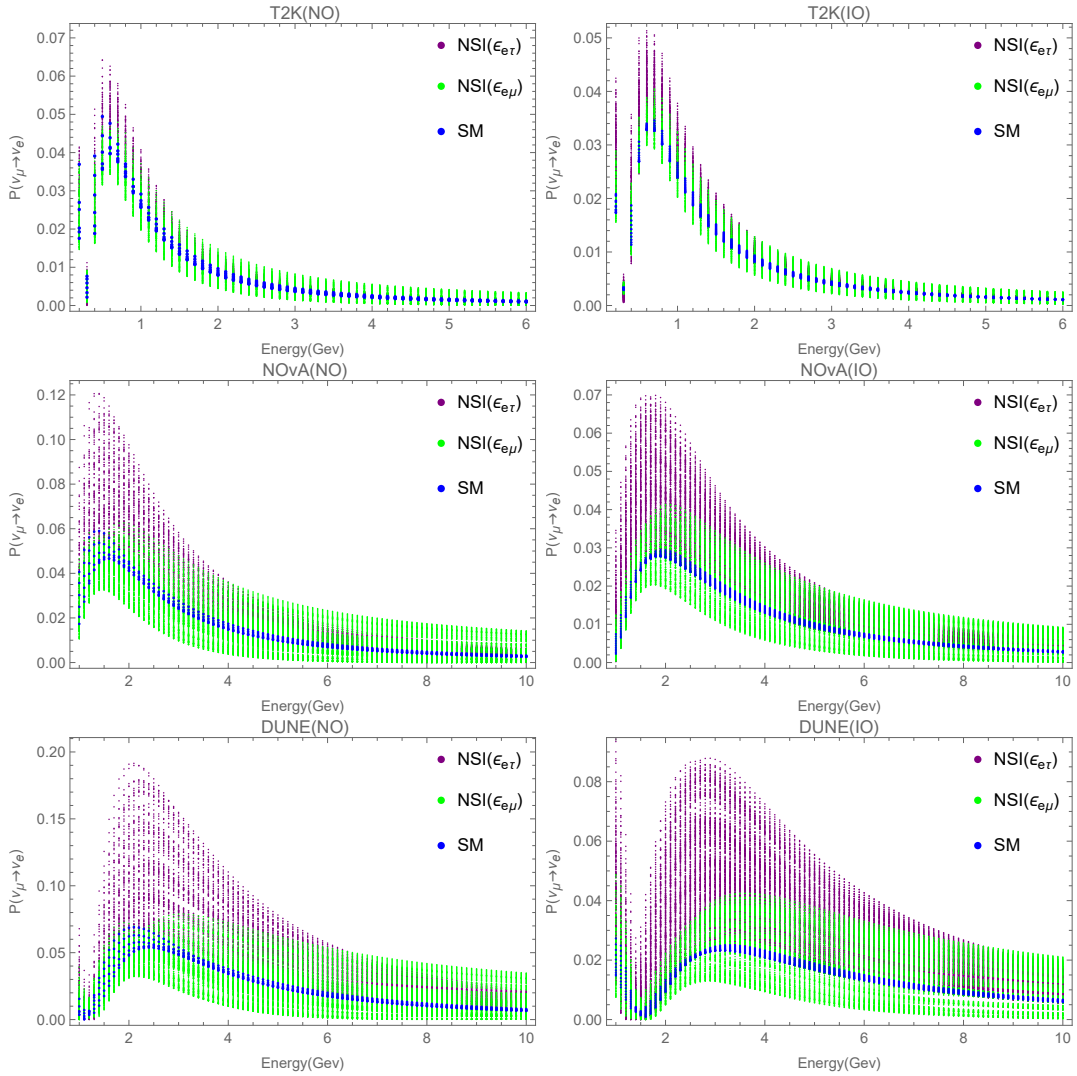

Figure 6.2.: Probability vs. neutrino energy for NO (left) and IO (right) in the T2K (upper), NOνA (middle), and DUNE (lower) experiments. The green band represents LGtI with a 1σ range of $\epsilon_{e\mu}$, $\phi_{e\mu}$, and cp phase; the purple band represents LGtI with 1σ an allowed range of $\epsilon_{e\tau}$, $\phi_{e\tau}$ and cp phase; and the blue band represents LGtI with 1σ an allowed range of cp phase.

Figure 6.2 illustrates the variation of probability $P_{\mu e}$ as a function of neutrino energy within 1σ range for SM and NSI scenarios in T2K, NOνA, and DUNE experiments. SM and NSI scenarios exhibit overlapping regions, so the effect becomes discernible primarily from the maxi-

Experiment	MO	Energy in GeV
DUNE	NO	[1, 1.5], [3.4, 10], [6, 10]
	IO	[1.2, 1.5], [1.7, 2.2]
NOνA	NO	[3.5, 10]
	IO	[6.5, 10]
T2K	NO	[0.2, 0.4], [1.3, 6]
	IO	[1.5, 6]

Table 6.3.: Specific range of energy where the temporal correlation parameter exceeds its classical limit, *i.e.* K_3 is violated for different mass ordering in SM and NSI scenarios.

mum deviation. For both ordering, the maximum deviation of $P_{\mu e}$ for the $\epsilon_{e\tau}$ scenario from SM is observed between $(1-3)$ GeV for NOvA and $(1.5-4.5)$ GeV for DUNE, while in IO, the $\epsilon_{e\mu}$ scenario also exhibits its maximum deviation within the same energy range. In the T2K experiment, it is hard to distinguish $P_{\mu e}$ for these scenarios for both NO and IO. For NO, the maximum deviation for the $\epsilon_{e\tau}$ scenario from SM in DUNE is ≈ 0.12 and ≈ 0.45 for $P_{\mu e}$ and K_3, respectively, while in NOνA, this deviation is ≈ 0.06 for $P_{\mu e}$ and ≈ 0.23 for K_3. For IO, the maximum deviation for the $\epsilon_{e\tau}$ scenario from SM, in the case of DUNE is ≈ 0.06 and ≈ 0.19 for $P_{\mu e}$ and K_3, respectively; similarly, in NOνA, the deviation is ≈ 0.04 for $P_{\mu e}$ and ≈ 0.1 for K_3. The maximum deviation for the $\epsilon_{e\mu}$ scenario from SM for DUNE is ≈ 0.02 and ≈ 0.07 for $P_{\mu e}$ and K_3, respectively, while in NOνA, the maximum deviation is ≈ 0.01 for $P_{\mu e}$ and ≈ 0.04 for K_3.
Probability serves as a fundamental measure in experimental observations, particularly in the context of neutrino oscillation studies, where it is commonly measured. LGtI can be expressed in terms of probabilities and exhibits complementary behavior to probabilities, providing an additional avenue to study the NSI effects. Hence, by initially detecting the NSI effects through probability measurements, we can reinforce their existence through LGtI observations. This dual approach strengthens our understanding of NSI phenomena and enhances our ability to characterize their impact on neutrino behavior. One advantage is that the possible deviation of NSI from SM is more pronounced in LGtI than in probabilities.

6.3 Conclusion

In this work, we studied the impact of $\epsilon_{e\mu}$ and $\epsilon_{e\tau}$ NSI scenarios on temporal correlation, which is measured by LGtI in the context of three-flavor neutrino oscillation, and compared the results with SM predictions across three distinct accelerator experiment setups. These two NSI scenarios have the potential to resolve tension that emerged in NOνA and T2K data. We look for the implication of new physics, whether the $\epsilon_{e\mu}$ or $\epsilon_{e\tau}$ NSI scenarios can be distinguished or not. We observed that in NO in the presence of NSI with $\epsilon_{e\tau}$, LGtI-violation was significantly enhanced in comparison to SM. The degree of enhancement in K_3 in DUNE surpasses that of NOvA. However, in the case of IO, LGtI violation is enhanced for the $\epsilon_{e\tau}$ scenario over SM interaction, while LGtI violation for the $\epsilon_{e\mu}$ scenario is not affected significantly. Therefore, an interesting result of this work is that if LGtI is violated in the DUNE experiment for IO at energy above 8.5 GeV, this would be possible only for the $\epsilon_{e\tau}$ scenario. The results of LGtI-violation for different NSI scenarios differ remarkably for DUNE. $\epsilon_{e\tau}$ scenario is favored in the context of normal ordering as well as inverted ordering. The possible deviation of NSI from SM is more pronounced in LGtI as compared to probabilities.